Cleavage of *tert*-Butyl Groups from the Tri-*tert*-butylphosphine Ligand in Osmium−Platinum Carbonyl Cluster Complexes

Richard D. Adams* and Erin Boswell

Department of Chemistry and Biochemistry, University of South Carolina, Columbia, South Carolina 29208

Received January 15, 2008

Two products, $Pt_2Os_3(CO)_{10}(PBu^t_3)(PBu^t_2CMe_2CH_2)(\mu\text{-H})$ (**1**) and $Pt_2Os_3(CO)_9(PBu^t_3)(\mu\text{-}PBu^t_2)(\mu\text{-H})(\mu_3\text{-}CCMe_2)$ (**2**), were obtained from the reaction of $Os_3(CO)_{12}$ with $Pt(PBu^t_3)_2$ at 97 °C. Compound **2** is new and consists of a square-pyramidal cluster of five metal atoms with a bridging PBu^t_2 ligand, a bridging hydrido ligand, and a triply bridging dimethylvinylidene ligand C═CMe_2 formed by transformations of a tri-*tert*-butylphosphine ligand. Compound **1** was transformed into **2** at 125 °C, and compound **2** was transformed into two new compounds, $PtOs_3(CO)_7(PBu^t_3)(\mu\text{-}PBu^t_2)(\mu_4\text{-CHCMeCH})$ (**3**) and $Pt_4Os_3(CO)_{12}(\mu\text{-}PBu^t_2)_2$ (**4**), at 174 °C. Compound **3** contains a bridging PBu^t_2 ligand and a quadruply bridging CHCMeCH ligand in a butterfly cluster of four metal atoms. Compound **4** contains four platinum atoms and three osmium atoms. The metal atoms are arranged in the form of a doubly capped square pyramid with the four platinum atoms in the square base. Two triangles of the square pyramid are capped by $Os(CO)_3$ groups. The molecule also contains two bridging di-*tert*-butylphosphido ligands on opposite sides of the Pt_4 square base. Compound **3** is electron-deficient by the amount of four electrons, and it reacts reversibly with CO to form the new compound $PtOs_3(CO)_8(PBu^t_3)(\mu\text{-}PBu^t_2)(\mu_4\text{-CHCMeCH})$ (**5**) by the addition of one CO ligand to the platinum atom. The electronic structures of **3**−**5** were investigated by Fenske–Hall molecular orbital calculations.

Introduction

The cleavage of hydrocarbon substituents from the phosphorus atoms of tertiary phosphines has been shown to be a leading the cause for catalyst deactivation when these ligands are used with metal complexes in homogeneous catalysis.[1] In recent studies we have shown that reactions of $Pt(PBu^t_3)_2$ and $Pd(PBu^t_3)_2$ with polynuclear metal carbonyl cluster complexes readily yield new mixed-metal cluster complexes under mild conditions that have $Pt(PBu^t_3)$ and $Pd(PBu^t_3)$ groups bridging the metal−metal bonds: e.g. eqs 1 and 2.

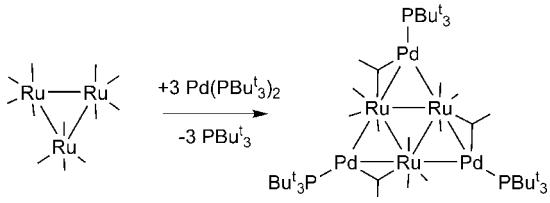

(1)

$Rh_4(CO)_{12}$ reacts with $Pd(PBu^t_3)_2$ to yield the higher nuclearity hexarhodium cluster complexes $Rh_6(CO)_{12}[Pd(PBu^t_3]_3$ and $Rh_6(CO)_{12}[Pd(PBu^t_3]_4$, which contain three and four edge-bridging $Pd(PBu^t_3)$ groups, respectively (eq 3).[4]

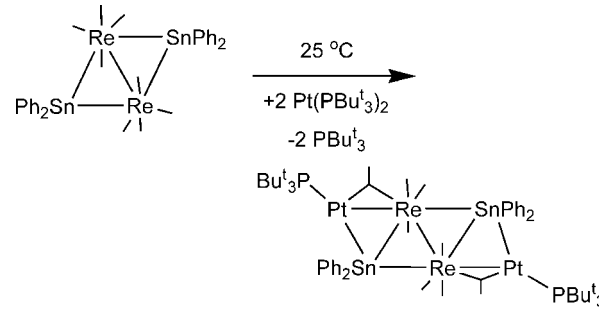

(2)

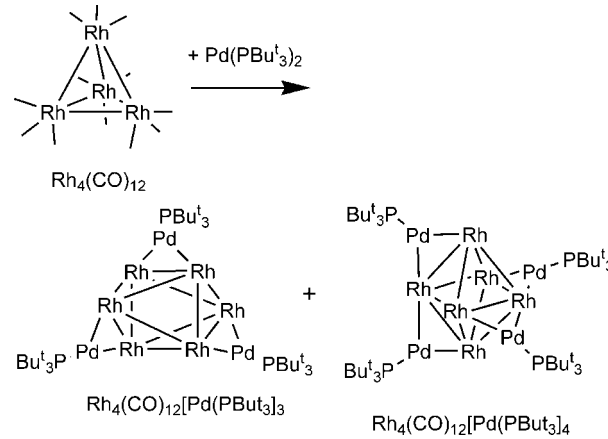

(3)

The reaction of $Os_3(CO)_{12}$ with $Pt(PBu^t_3)_2$ yielded three products formed by the sequential addition of one to three

* To whom correspondence should be addressed. E-mail:Adams@mail.chem.sc.edu.

(1) (a) Garrou, P. E. *Chem. Rev.* **1985**, *85*, 171–185. (b) Dubois, R. A.; Garrou, P. E. *Organometallics* **1986**, *5*, 460–466. (c) Lavigne, G. In *Chemistry of Metal Cluster Complexes*; Shriver, D. F., Kaesz, H. D., Adams, R. D., Eds., VCH: Weinheim, Germany, 1990; pp 201–303.

(2) Adams, R. D.; Captain, B.; Fu, W.; Hall, M. B.; Manson, J.; Smith, M. D.; Webster, C. E. *J. Am. Chem. Soc.* **2004**, *126*, 5253–5267.

(3) Adams, R. D.; Captain, B.; Herber, R. H.; Johansson, M.; Nowik, I.; Smith, J. L., Jr.; Smith, M. D. *Inorg. Chem.,* **2005**, *44*, 6346–6358.

(4) Adams, R. D.; Captain, B.; Zhu, L. *J. Cluster Sci.* **2004**, *15*, 139–149.

10.1021/om8000422 CCC: $40.75
Publication on Web 04/05/2008

$Pt(PBu^t_3)$ groups to the three Os−Os bonds of the original triangular triosmium cluster (eq 4).[5]

It has been shown the *tert*-butyl groups on PBu^t_3 ligands can undergo CH activation by metal atoms on the methyl groups[5,6] and can also be cleaved entirely from the phosphorus atom to yield bridging di-*tert*-butylphosphido ligands, PBu^t_2.[7]

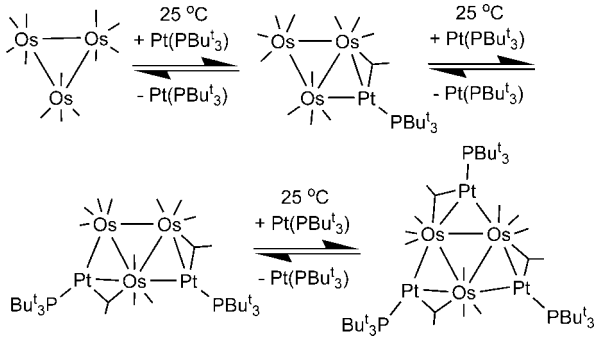

(4)

We have now investigated the reactions of $Os_3(CO)_{12}$ with $Pt(PBu^t_3)_2$ at elevated temperatures, and we have obtained a number of new platinum−osmium carbonyl cluster complexes containing bridging di-*tert*-butylphosphido ligands. In certain cases we have observed the cleavage of the *tert*-butyl group from the PBu^t_3 ligand and some of the features of what has happened to the cleaved *tert*-butyl group. These results are reported herein.

Experimental Section

General Data. All the reactions were performed under a nitrogen atmosphere by using Schlenk techniques. Reagent grade solvents were dried by the standard procedures and were freshly distilled prior to use. Infrared spectra were recorded on an AVATAR 360 FT-IR spectrophotometer. ^{1}H NMR and $^{31}P\{^1H\}$ NMR spectra were recorded on a Varian Mercury 400 spectrometer operating at 400 and 162 MHz, respectively. $^{31}P\{^1H\}$ NMR spectra were externally referenced against 85% *o*-H_3PO_4. Mass spectrometric measurements performed by direct exposure probe using electron impact ionization (EI) were carried out on a VG 70S instrument. $Os_3(CO)_{12}$ was prepared by a previously reported procedure.[8] $Pt(PBu^t_3)_2$ was purchased from STREM and was used without further purification. Nonane (99%) and decane (99%) were received from Alfa Aesar and used without further purification. Product separations were performed by TLC in air by using Analtech 0.25, 0.5, or 1.0 mm silica gel 60 Å F_{254} glass plates.

Reaction of $Os_3(CO)_{12}$ with $Pt(PBu^t_3)_2$ at 97 °C. A 15 mg amount (0.017 mmol) of $Os_3(CO)_{12}$ was dissolved in 15 mL of distilled heptane in a 50 mL three-neck flask. A 50 mg portion (0.083 mmol) of $Pt(PBu^t_3)_2$ was added, and the reaction mixture was heated to reflux for 5 h. The solvent was then removed in vacuo and the residue extracted with methylene chloride and separated by TLC using a 4/1 (v/v) hexane/methylene chloride solvent mixture to yield in order of elution 1.0 mg (3%) of red $Pt_2Os_3(CO)_9(PBu^t_3)(\mu\text{-}PBu^t_2)(\mu\text{-}H)(\mu_3\text{-}CCMe_2)$ (**2**) and 5.0 mg (18%) of the previously reported brown $Pt_2Os_3(CO)_{10}(PBu^t_3)(PBu^t_2CMe_2CH_2)(\mu\text{-}H)$ (**1**).[5] Spectral data for **2**: IR ν_{CO} (cm^{-1}, in CH_2Cl_2) 2046 (m), 2012 (vs), 1995 (m, sh), 1956 (m), 1770 (w); ^{1}H NMR (ppm, in C_6D_6) δ 1.14 (d, 9H, $^2J_{P-H}$ = 14 Hz), 1.25 (d, 9H, $^2J_{P-H}$ = 14 Hz), 1.38 (d, 27H, $^2J_{P-H}$ = 12 Hz), 2.16 (s, br, 6H), –20.26 (d, 1H, $^2J_{P-H}$ = 8 Hz); ^{1}H NMR (ppm, in $CDCl_3$ at –50 °C) δ 2.735 (s, 3H), 2.617 (s, 3H), 1.375 (d, 27H, $^3J_{P-H}$ = 12 Hz), 0.888 (d, 9H, $^3J_{P-H}$ = 7 Hz), 0.787 (d, 9H, $^3J_{P-H}$ = 11 Hz), –20.897 (d, 1H, $^2J_{P-H}$ = 4 Hz); ^{31}P NMR (ppm, in C_6D_6) δ 127.09 (s, 1P, $^1J_{Pt-P}$ = 5577 Hz, $^3J_{Pt-P}$ = 41 Hz), 380.5 (s, 1P, $^1J_{Pt-P}$ = 81 Hz). EI/MS (*m*/*z*): M, 1616; M − CO, 1588; M − 2CO, 1560; M − 3CO, 1532; M − 4CO, 1504.

Reaction of $Os_3(CO)_{12}$ with $Pt(PBu^t_3)_2$ at 125 °C. A 15 mg portion (0.017 mmol) of $Os_3(CO)_{12}$ was dissolved in 15 mL of distilled octane in a 50 mL three-neck flask. A 50 mg amount (0.083 mmol) of $Pt(PBu^t_3)_2$ was added, and the reaction mixture was heated to reflux for 2.5 h. The solvent was then removed in vacuo and the residue extracted with methylene chloride and separated by TLC using a 4/1 (v/v) hexane/methylene chloride solvent mixture to yield in order of elution 1.1 mg (4%) of green $PtOs_3(CO)_7(PBu^t_3)(\mu\text{-}PBu^t_2)(\mu_4\text{-}CHCMeCH)$ (**3**), 3.3 mg (12%) of red **2**, and 1.1 mg (3%) of purple $Pt_4Os_3(CO)_{12}(\mu\text{-}PBu^t_2)_2$ (**4**). Spectral data for **3**: IR ν_{CO} (cm^{-1}, in CH_2Cl_2) 2052 (s), 1992 (vs), 1979 (s), 1966 (s), 1924 (m), 1898 (m); ^{1}H NMR (ppm, in C_6D_6) δ 1.26 (d, 27H, $^2J_{P-H}$ = 12 Hz), 1.31 (d, 9H, $^2J_{P-H}$ = 14 Hz), 1.54 (d, 9H, $^2J_{P-H}$ = 14 Hz), 2.40 (d, 3H, $^4J_{P-H}$ = 1 Hz), 2.83 (dd, 1H, $^3J_{P-H}$ = 3 Hz, $^4J_{P-H}$ = 1 Hz), 8.19 (dd, 1H, $^3J_{P-H}$ = 2 Hz, $^3J_{P-H}$ = 1 Hz); ^{31}P NMR (ppm, in $CDCl_3$) δ 91.0 (s, 1P, $^1J_{Pt-P}$ = 4003 Hz), 259.73 (s, 1P, $^2J_{Pt-P}$ = 316 Hz). EI/MS (*m*/*z*): M, 1362; M − 2CO, 1306; M − 3CO, 1278; M − 4CO, 1250. Spectral data for **4**: IR ν_{CO} (cm^{-1}, in CH_2Cl_2) 2071 (w), 2047 (vs), 2025 (m, sh), 2015 (s), 1995 (m), 1984 (m), 1960 (w); ^{1}H NMR (ppm, in C_6D_6) δ 0.85 (d, 18H, $^2J_{P-H}$ = 8 Hz), 0.89 (d, 18H, $^2J_{P-H}$ = 8 Hz); ^{31}P NMR (ppm, in C_6D_6) δ 303.4 (s, 2P, $^1J_{Pt-P}$ = 1412 Hz). EI/MS (*m*/*z*): M, 1997; M − 4CO, 1865; M − 5CO, 1837.

Reaction of $Os_3(CO)_{12}$ with $Pt(PBu^t_3)_2$ at 150 °C. A 15 mg portion (0.017 mmol) of $Os_3(CO)_{12}$ was dissolved in 15 mL of nonane in a 50 mL three-neck flask. A 50 mg amount (0.083 mmol) of $Pt(PBu^t_3)_2$ was added, and the reaction mixture was heated to reflux for 5 h. The solvent was then removed in vacuo and the residue extracted with methylene chloride and separated by TLC using a 4/1 (v/v) hexane/methylene chloride solvent mixture to yield in order of elution 4.0 mg (17%) of green **3**, 1.1 mg (4%) of red **2**, and 1.0 mg (3%) of purple **4**.

Conversion of 1 to 2. A 5.0 mg (0.0030 mmol) amount of **1** was dissolved in 10 mL of distilled octane and the mixture heated to reflux for 1.5 h. The solvent was removed in vacuo and the residue extracted with methylene chloride and separated by TLC using a 4/1 (v/v) hexane/methylene chloride solvent mixture to yield 1.5 mg (30%) of **2**.

Conversion of 2 to 3 and 4. A 10 mg amount (0.006 mmol) of **2** was dissolved in 15 mL of decane and the mixture heated to reflux for 2 h. The solvent was removed in vacuo and the residue extracted with methylene chloride and separated by TLC using a 4/1 (v/v) hexane/methylene chloride solvent mixture to yield in order of elution 2.0 mg of **3** (23%) and 1.6 mg of **4** (13%).

Reaction of 3 with CO. A 12.0 mg (0.009 mmol) amount of **3** was dissolved in 15 mL of hexane. CO gas was bubbled through the solution for 2 h at 25 °C. The solvent was removed in vacuo and the residue extracted with methylene chloride and separated by TLC using a 4/1 (v/v) hexane/methylene chloride solvent mixture to yield in order of elution 3.0 mg of unreacted **3** and 6.7 mg (54%) of orange $PtOs_3(CO)_8(PBu^t_3)(\mu\text{-}PBu^t_2)(\mu_4\text{-}CHCMeCH)$ (**5**). Spectral data for **5**: IR ν_{CO} (cm^{-1}, in CH_2Cl_2) 2055 (vs), 2005 (m), 1992 (s), 1979 (s), 1965 (s), 1925 (m), 1897 (w); ^{1}H NMR (ppm, in C_6D_6) δ 1.07 (d, 27H, $^2J_{P-H}$ = 12 Hz), 1.33 (d, 9H, $^2J_{P-H}$ = 14

(5) Adams, R. D.; Captain, B.; Zhu, L. *Inorg. Chem.* **2006**, *45*, 430–436.

(6) (a) Goel, A. B.; Goel, S.; Van Derveer, D. *Inorg. Chim. Acta* **1981**, *54*, L267–L268. (b) Goel, A. B.; Goel, S.; Van Derveer, D. *Inorg. Chim. Acta* **1984**, *82*, L9–L10. (c) Mullica, D. F.; Sappenfield, E. L.; Leschnitzer, D. H. *Acta Crystallogr., Sect. C: Cryst. Struct. Commun.* **1991**, *47*, 874–876. (d) Goel, A. B.; Goel, S.; Van Derveer, D.; Clark, H. C. *Inorg. Chim. Acta* **1981**, *53*, L117–L118.

(7) (a) Goel, A. B.; Goel, S. *Inorg. Chim. Acta* **1984**, *90*, L33–L34. (b) Adams, R. D.; Captain, B. *Organometallics* **2007**, *26*, 6564–6575. (c) Adams, R. D.; Boswell, E.; Captain, B.; Zhu, L. *J. Cluster Sci.*, in press.

(8) Johnson, B. F. G.; Lewis, J. *Inorg. Synth.* **1972**, *13*, 93.

Table 1. Crystallographic Data for Compounds 2–5

	2	3	4	5
empirical formula	$Os_3Pt_2P_2O_9C_{33}H_{52}$	$Os_3PtP_2O_7C_{31}H_{50}$	$Os_3Pt_4P_2O_{12}C_{28}H_{36}$	$Os_3PtP_2O_8C_{32}H_{50}$
formula wt	1615.47	1362.34	1977.47	1390.35
cryst syst	monoclinic	monoclinic	monoclinic	monoclinic
lattice params				
a (Å)	15.303(2)	13.7017(7)	33.720(8)	9.1635(5)
b (Å)	13.415(2)	10.4238(5)	14.1815(8)	25.162(4)
c (Å)	24.337(4)	26.776(4)	19.736(1)	17.668(1)
α (deg)	90	90	90	90
β (deg)	95.975(3)	96.779(1)	102.095(1)	101.637(1)
γ (deg)	90	90	90	90
V (Å^3)	4968.8(12)	3797.6(3)	9228.3(9)	3990.1(4)
space group	$P2_1/c$ (No. 14)	$P2_1/c$ (No. 14)	$C2/c$ (No. 15)	$P2_1/n$ (No. 14)
Z	4	4	8	4
ρ_{calcd} (g/cm^3)	2.16	2.38	2.85	2.31
μ(Mo Kα) (mm^{-1})	13.36	13.80	20.42	13.14
temp (K)	294(2)	294(2)	294(2)	294(2)
$2\theta_{max}$ (deg)	56.56	56.60	50.06	56.68
no. of obsd rflns ($I > 2\sigma(I)$)	9041	8142	5713	6938
no. of params	463	413	454	431
goodness of fit (GOF)[a]	1.099	1.136	0.939	1.055
max shift final cycle	0.001	0.002	0.002	0.001
residuals:[a] R1; wR2	0.0459; 0.1264	0.0317; 0.0795	0.0405; 0.0856	0.0451; 0.0881
abs cor, max/min	1.000/0.074	1.000/0.532	1.000/0.290	1.000/0.647
largest peak in final diff map (e/Å^3)	2.70	2.36	1.48	1.31

[a] $R1 = \sum_{hkl}(||F_o| - |F_c||)/\sum_{hkl}|F_o|$; $wR2 = [\sum_{hkl}w(|F_o| - |F_c|)^2/\sum_{hkl}wF_o^2]^{1/2}$, $w = 1/\sigma^2(F_o)$; $GOF = [\sum_{hkl}w(|F_o| - |F_c|)^2/(n_{data}-n_{vari})]^{1/2}$.

Hz), 1.54 (d, 9H, $^2J_{P-H} = 15$ Hz), 2.86 (s, 3H), 3.88 (dd, 1H, $^3J_{P-H} = 2$ Hz, $^4J_{P-H} = 2$ Hz), 8.81 (dd, 1H, $^3J_{P-H} = 2$ Hz, $^3J_{P-H} = 2$ Hz); ^{31}P NMR (ppm, in C_6D_6) δ 110.84 (d, 1P, $^3J_{P-P} = 7$ Hz, $^1J_{Pt-P} = 2381$ Hz). 261.78 (d, 1P, $^3J_{P-P} = 8$ Hz, $^2J_{Pt-P} = 155$ Hz). EI/MS (*m*/*z*): M, 1390; M − CO, 1362; M − 2CO, 1334; M − 3CO, 1306; M − 4CO, 1278.

Conversion of 5 to 3. An 8.0 mg (0.006 mmol) amount of **5** was dissolved in 10 mL of octane and the mixture heated to reflux for 2 h. The solvent was removed in vacuo and the residue extracted with methylene chloride and separated by TLC using a 4/1 (v/v) hexane/methylene chloride solvent mixture to yield 3.0 mg of **3** (38%).

Crystallographic Analyses. Red single crystals of **2** suitable for diffraction analysis were grown by slow evaporation of solvent from methylene chloride/hexane solution at –25 °C. Dark single crystals of **3** were grown by slow evaporation of solvent from a diethyl ether/octane solution at –25 °C. Dark single crystals of **4** were grown by slow evaporation of solvent from toluene/octane solution at –25 °C. Orange single crystals of **5** were grown by slow evaporation of solvent from benzene/octane solution at 7 °C.

Each data crystal was glued onto the end of a thin glass fiber. X-ray intensity data were measured using a Bruker SMART APEX CCD-based diffractometer using Mo Kα radiation ($\lambda = 0.710\,73$ Å). The raw data frames were integrated with the SAINT+ program by using a narrow-frame integration algorithm.[9] Corrections for the Lorentz and polarization effects were also applied by SAINT. An empirical absorption correction based on the multiple measurement of equivalent reflections was applied by using the program SADABS. All structures were solved by a combination of direct methods and difference Fourier syntheses and refined by full-matrix least squares on F^2, by using the SHELXTL software package.[10] Unless indicated otherwise, all hydrogen atoms were placed in geometrically idealized positions and included as standard riding atoms. Crystal data, data collection parameters, and results of the analyses for compounds are given in Table 1.

Compound **2** crystallized in the monoclinic crystal system. The systematic absences in the intensity data were consistent with the unique space group $P2_1/c$. The hydrido ligand was located and refined with isotropic thermal parameters. Compound **3** crystallized in the monoclinic crystal system. The systematic absences in the intensity data were consistent with the unique space group $P2_1/c$.

Compound **4** crystallized in the monoclinic crystal system. The systematic absences in the intensity data were consistent with the space group $C2/c$. There is a region of disorder in the asymmetric unit. On the basis of several trial models, the disordered species appear to be fractionally occupied octane molecules. No satisfactory disorder model could be obtained, despite much effort. The solvent-containing volume constitutes 1398.3 Å^3, or 15% of the total unit cell volume. The contribution of the disordered species (619 electrons per unit cell) was removed from subsequent structure factor calculations with SQUEEZE.[11] Note that the final tabulated MW, d_{calcd}, and $F(000)$ values refer to the crystallographically identifiable species only.

Compound **5** crystallized in the monoclinic crystal system. The systematic absences in the intensity data were consistent with the unique space group $P2_1/n$. All non-hydrogen atoms were refined with anisotropic thermal parameters. The hydrogen atoms on the *tert*-butyl groups were calculated by assuming standard geometries and were included as fixed contributions on the final cycles of refinement.

Molecular Orbital Calculations. Molecular orbital calculations reported here were performed by the Fenske–Hall method.[12] These calculations utilize a graphical user interface developed[13] to build inputs and view outputs from standalone Fenske–Hall (version 0.1.v117) and MOPLOT2[14] binary executables. Contracted Clementi double-ζ basis sets were used for the Os 5d, Pt 5d, P 3p, and C and O 2p atomic orbitals. The Fenske–Hall scheme is a nonempirical,

(9) SAINT+, Version 6.2a; Bruker Analytical X-ray Systems, Madison, WI, 2001.

(10) Sheldrick, G. M. SHELXTL, Version 6.1; Bruker Analytical X-ray Systems, Madison, WI, 1997.

(11) Spek, A. L. PLATON, A Multipurpose Crystallographic Tool; Utrecht University, Utrecht, The Netherlands, 1998.

(12) (a) Hall, M. B.; Fenske, R. F. *Inorg. Chem.* **1972**, *11*, 768–775. (b) Webster, C. E.; Hall, M. B. In *Theory and Applications of Computational Chemistry: The First Forty Years*; Dykstra, C., Ed.; Elsevier: Amsterdam, 2005; Chapter 40, pp 1143–1165.

(13) Manson, J.; Webster, C. E.; Hall, M. B. JIMP, Development Version 0.1.v117 (built for Windows PC and Redhat Linux); Department of Chemistry, Texas A&M University, College Station, TX 77842; http://www.chem.tamu.edu/jimp/.

(14) Lichtenberger, D. L. MOPLOT2: for Orbital and Density Plots from Linear Combinations of Slater or Gaussian Type Orbitals, Version 2.0; Department of Chemistry, University of Arizona, Tucson, AZ 85721, 1993.

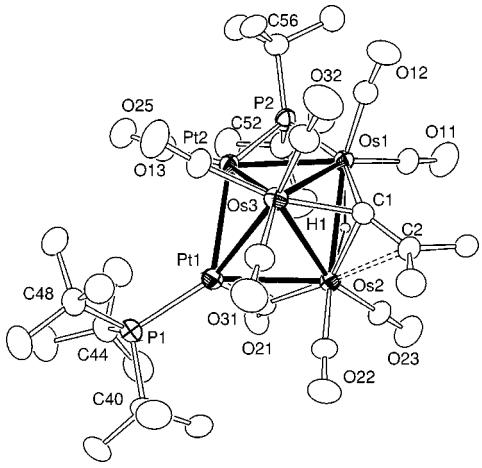

Figure 1. ORTEP diagram of **2** showing thermal ellipsoids at the 40% probability level. The hydrogen atoms on the methyl groups are omitted for clarity.

approximate method that is capable of calculating molecular orbitals for very heavy transition-metal systems and has built-in fragment analysis routines that also allow one to assemble transition-metal cluster structures from the ligand-containing fragments. In these calculations, PH_3 was used in place of the PBu^t_3 ligand, PH_2 was used in place of the bridging PBu^t_2 ligand, P−H = 1.41 Å, and the methyl group on the bridging CHCMeCH ligand was replaced with a hydrogen atom with C−H = 0.95 Å.

Results and Discussion

Two products, $Pt_2Os_3(CO)_{10}(PBu^t_3)(PBu^t_2CMe_2CH_2)(\mu\text{-H})$ (**1**; 18% yield) and $Pt_2Os_3(CO)_9(PBu^t_3)(\mu\text{-}PBu^t_2)(\mu\text{-H})(\mu_3\text{-}CCMe_2)$ (**2**; 3% yield) were obtained from the reaction of $Os_3(CO)_{12}$ with $Pt(PBu^t_3)_2$ when heated to reflux in a heptane solution for 5 h (eq 5).

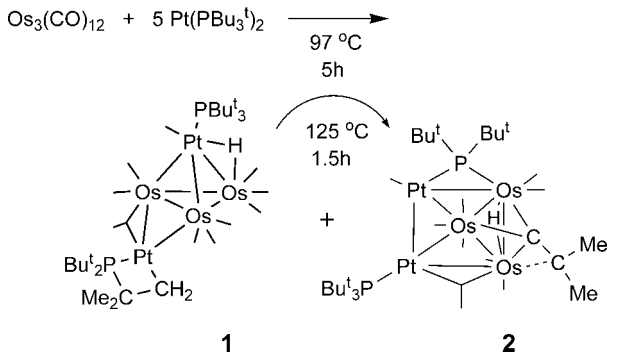

(5)

Compound **1** was obtained previously in a better yield (22%) from the reaction of $Os_3(CO)_{12}$ with $Pt(PBu^t_3)_2$ at a lower temperature (in hexane solvent at reflux).[5] Compound **2** is new and has been characterized by a combination of IR and NMR spectroscopy, mass spectrometry, and single-crystal X-ray diffraction analysis. An ORTEP diagram of the molecular structure of **2** is shown in Figure 1. Selected bond distances and angles for **2** are given in Tables 2 and 3. The structure of **2** consists of a square-pyramidal cluster of five metal atoms: three of osmium and two of platinum. The two platinum atoms and two of the osmium atoms define the "square" base, and one of the osmium atoms, Os(3), occupies the apical position of the pyramid. The molecule contains nine carbonyl ligands. Three of these are terminal ligands

Table 2. Selected Intramolecular Bond Distances for 2 and 4[a]

2			4		
atom	atom	dist (Å)	atom	atom	dist (Å)
Pt(1)	Os(2)	2.8027(6)	Pt(1)	Pt(2)	3.0390(8)
Pt(1)	Pt(2)	2.8719(6)	Pt(2)	Pt(3)	2.6537(7)
Os(1)	Pt(2)	2.7674(6)	Pt(3)	Pt(4)	3.1013(7)
Os(1)	Os(2)	2.9338(6)	Pt(1)	Pt(4)	2.6567(7)
Pt(1)	Os(3)	2.8344(7)	Os(2)	Pt(1)	2.7496(8)
Pt(2)	Os(3)	2.7372(7)	Os(2)	Pt(2)	2.7667(7)
Os(1)	Os(3)	2.8503(6)	Os(1)	Os(2)	2.6624(7)
Os(2)	Os(3)	2.8833(6)	Os(3)	Pt(3)	2.7483(7)
Os(1)	H(1)	1.76(2)	Os(3)	Pt(4)	2.7597(8)
Os(2)	H(1)	1.75(2)	Os(1)	Os(3)	2.6613(7)
Os(1)	C(1)	2.11(1)	Os(1)	Pt(1)	2.6570(8)
Os(2)	C(1)	2.13(1)	Os(1)	Pt(2)	2.6645(7)
Os(3)	C(1)	2.10(1)	Os(1)	Pt(3)	2.6529(7)
Os(2)	C(2)	2.508(10)	Os(1)	Pt(4)	2.6563(7)
C(1)	C(2)	1.375(14)			

[a] Estimated standard deviations in the least significant figure are given in parentheses.

on Os(3). Os(1) and Os(2) each have two terminal CO ligands. Pt(2) contains one terminal CO ligand, and there is a bridging CO ligand, C(21)−O(21), across the Pt(1)−Os(2) bond. There is one PBu^t_3 that is coordinated to Pt(1), one PBu^t_2 ligand that bridges the Os(1)−Pt(2) bond, and a dimethylvinylidene ligand that bridges the triangular group of three osmium atoms. Bridging vinylidene ligands are not uncommon in cluster chemistry.[15] The carbon atom C(1) is bonded to all three osmium atoms (Os(1)−C(1) = 2.111(10) Å, Os(2)−C(1) = 2.135(10) Å, and Os(3)−C(1) = 2.098(10) Å), while the carbon C(2) that is bonded to C(1) is bonded to Os(2) at a much longer distance (Os(2)−C(2) = 2.508(10) Å). As expected, the short C(1)−C(2) bond distance, 1.375(14) Å, reflects the C−C double-bond character of this bond. Compound **2** also contains one bridging hydrido ligand (H(1)) that was located and refined in the structural analysis (Os(1)−H(1) = 1.76(2) Å and Os(2)−H(1) = 1.75(2) Å). The hydrido ligand exhibits the expected high-field resonance shift in the ^{1}H NMR spectrum: δ –20.26 (d, 1H, $^2J_{P-H}$ = 8 Hz). The Os−Os bond distances (Os(1)−Os(3) = 2.8503(6) Å and Os(2)−Os(3) = 2.8833(6) Å) are similar to the average of the Os−Os bond distances observed in $Os_3(CO)_{12}$ (2.877(3) Å).[16] The Os(1)−Os(2) bond is significantly longer than the other two (2.9338(6) Å), likely due to the presence of the bridging hydrido ligand H(1).[17] The methyl groups on C(2) appear as a single broad resonance at 2.16 ppm in the ^{1}H NMR spectrum at room temperature. As we suspected dynamic activity, a variable-temperature NMR study was performed on this compound, which confirmed a dynamic exchange process. The broad resonance resolved into two sharp singlets at –50 °C (δ 2.74 and 2.62) which coalesced and re-formed as a sharp singlet on heating to +50 °C. From the coalescence temperature 5 °C, it was possible to calculate the $\Delta G^{\ddagger}$ value of activation for the exchange process, which is 13.4(2) kcal/mol at 278 K. As noted above, the Os(2)−C(2) bond is quite long and presumably weak. Thus, the exchange of the methyl groups on C(2) could occur simply by breaking the Os(2)−C(2) bond, rotating about the C(1)−C(2) vector, and then re-forming the Os(2)−C(2) bond.

Compound **1** is a precursor to **2**, as it was converted into **2** in 30% yield by heating it to reflux in octane solvent for 1.5 h. This supports the notion that the vinylidene ligand is derived from a *tert*-butyl group of a PBu^t_3 ligand by cleavage of the P−C bond and abstraction of three hydrogen atoms from one

(15) Bruce, M. I. *Chem. Rev.* **1991**, *91*, 197–257.
(16) Churchill, M. R.; DeBoer, B. G. *Inorg. Chem.* **1977**, *16*, 878–884.
(17) Teller, R. G.; Bau, R. *Struct. Bonding (Berlin)* **1981**, *41*, 1–82.

Table 3. Selected Intramolecular Bond Angles for 2 and 4[a]

2				4			
atom	atom	atom	angle (deg)	atom	atom	atom	angle (deg)
Pt(1)	Pt(2)	Os(1)	98.29(8)	Pt(1)	Pt(2)	Pt(3)	92.31(2)
Pt(2)	Os(1)	Os(2)	81.87(7)	Pt(2)	Pt(3)	Pt(4)	87.70(2)
Os(1)	Os(2)	Pt(1)	96.07(7)	Pt(3)	Pt(4)	Pt(1)	90.87(2)
Os(2)	Os(3)/Os(3)	Pt(2)	82.38(6)	Pt(4)	Pt(1)	Pt(2)	88.96(2)
Pt(1)	Os(3)	Pt(2)	62.03(5)	Os(2)	Os(1)	Os(3)	173.75(3)
Pt(2)	Os(3)	Os(1)	59.34(5)	Pt(1)	Os(2)	Pt(2)	66.86(2)
Os(1)	Os(3)	Os(2)	61.55(6)	Pt(1)	Os(1)	Pt(2)	69.65(2)
Os(2)	Os(3)	Pt(1)	58.70(5)	Pt(2)	Os(1)	Pt(3)	59.88(9)
Pt(1)	Os(3)	Os(1)	97.26(7)	Pt(3)	Os(3)	Pt(4)	68.53(2)
Pt(2)		Os(2)	83.32(6)	Pt(4)	Os(1)	Pt(1)	60.00(9)
				Pt(2)	Os(1)	Pt(4)	97.49(2)
				Pt(1)	Os(1)	Pt(3)	101.58(2)
				Pt(3)	Os(1)	Pt(4)	71.48(2)

[a] Estimated standard deviations in the least significant figure are given in parentheses.

of its methyl groups. The remnant PBu^t_2 group and one of the hydrogen atoms are still present in **2** as bridging ligands. The fate of the other two hydrogen atoms is not known. It appears that the first step in the cleavage of the *tert*-butyl group from the phosphorus atom is the metalation of one of the methyl groups, as observed in compound **1**. The sequence of the remaining transformations was not determined in this work.

When $Os_3(CO)_{12}$ was allowed to react with $Pt(PBu^t_3)_2$ at a slightly higher temperature (octane reflux), compound **2** was obtained in a better yield (12%) along with two new compounds, $PtOs_3(PBu^t_3)(\mu\text{-}PBu^t_2)(\mu_4\text{-}CHCMeCH)(CO)_7$ (**3**; 4% yield) and $Pt_4Os_3(CO)_{12}(\mu\text{-}PBu^t_2)_2$ (**4**; 3% yield) (eq 6).

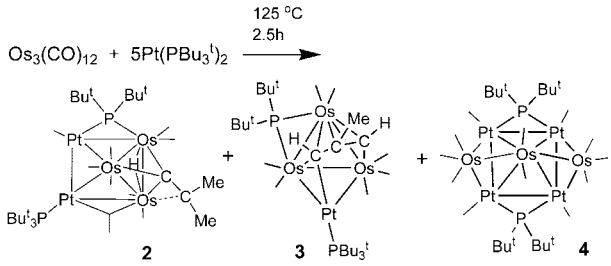

(6)

Compounds **3** and **4** have been characterized by a combination of IR and NMR spectroscopy, mass spectrometry, and single crystal X-ray diffraction analysis. An ORTEP diagram of the molecular structure of **3** is shown in Figure 2. Selected bond distances and angles for **3** are given in Tables 4 and 5. Compound **3** contains only four metal atoms,: three of osmium and one of platinum arranged in the form of a butterfly geometry. The platinum atom in a "wingtip" site bridges one edge of a triangular group of the three osmium atoms. One of the Os−Os bonds (Os(2)−Os(3) = 2.7511(3) Å) is significantly shorter than the other two (Os(1)−Os(2) = 2.8767(3) Å and Os(1)−Os(3) = 2.9605(3) Å). The shortness of this bond can be attributed to the presence of a bridging PBu^t_2 ligand. The molecule contains one PBu^t_3 ligand that is coordinated to the platinum atom, and there are seven terminal CO ligands that are coordinated to the osmium atoms, as shown in Figure 2. The most interesting feature in **3** is a CHCMeCH ligand that could be described as a dimetalla-2-methylallyl group that bridges all four metal atoms. Triply bridging dimetallaallyl ligands are quite common. Some classic examples are found in the complexes $Os_3(CO)_9(\mu_3\text{-}MeCCHCMe)(\mu\text{-}H)$[18] and $Os_3(CO)_9(\mu_3\text{-}MeCCHCH)(\mu\text{-}H)$[19] and $Os_4(CO)_{11}(\mu_3\text{-}MeCCHCH)(\mu\text{-}H)$.[19] The atom C(1) in **3** is unusual because it is bonded to three metal atoms, one hydrogen atom, and one carbon atom C(2): Os(2)−C(1) = 2.270(6) Å, Os(3)−C(1) = 2.348(6) Å, and Pt(1)−C(1) = 2.088 Å. The bonding is clearly delocalized and will be explained further by molecular orbital calculations that will be described below. Quadruply bridging dimetallaallyl ligands are rare. Two interesting examples include the anionic nonasomium complex $[Os_9(CO)_{21}(\mu_4\text{-}HCCMeCH)]^-$ and the pentaruthenium

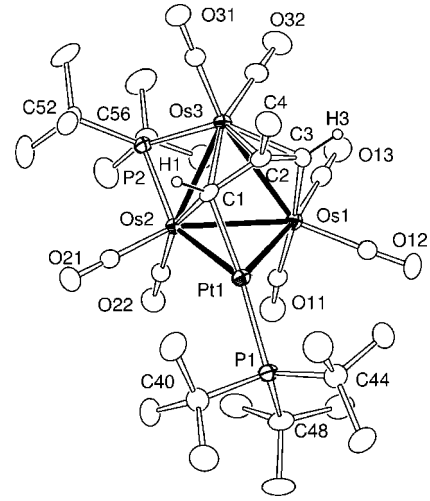

Figure 2. ORTEP diagram of **3** showing thermal ellipsoids at the 40% probability level. The hydrogen atoms on the methyl groups are omitted for clarity.

Table 4. Selected Intramolecular Bond Distances for 3 and 5[a]

3			5		
atom	atom	dist (Å)	atom	atom	dist (Å)
Os(1)	Os(2)	2.8767(3)	Os(1)	Os(2)	2.8455(6)
Os(2)	Os(3)	2.7511(3)	Os(2)	Os(3)	2.7279(5)
Os(1)	Os(3)	2.9605(3)	Os(1)	Os(3)	2.9527(6)
Os(1)	Pt(1)	2.7763(3)	Os(1)	Pt(1)	2.7915(6)
Os(2)	Pt(1)	2.6970(3)	Os(2)	Pt(1)	2.7384(6)
Os(1)	C(3)	2.123(6)	Os(1)	C(3)	2.11(1)
Os(3)	C(3)	2.226(6)	Os(3)	C(3)	2.21(1)
Os(3)	C(2)	2.255(6)	Os(3)	C(2)	2.22(1)
Os(3)	C(1)	2.348(6)	Os(3)	C(1)	2.370(9)
Os(2)	C(1)	2.270(6)	Os(2)	C(1)	2.29(1)

[a] Estimated standard deviations in the least significant figure are given in parentheses.

(18) Catiglioni, M.; Giordano, R.; Sappa, E. *J. Chem. Soc., Dalton Trans.* **1986**, 23–30.

(19) Hong, C.; Johnson, B. F. G.; Lewis, J.; Braga, D.; Grepioni, F. *J. Organomet. Chem.* **1990**, *398*, 159–164.

Table 5. Selected Intramolecular Bond Angles for 3 and 5[a]

3				5			
atom	atom	atom	angle (deg)	atom	atom	atom	angle (deg)
Os(1)	Os(2)	Os(3)	63.432(8)	Os(1)	Os(2)	Os(3)	63.92(6)
Os(2)	Os(3)	Os(1)	60.353(8)	Os(2)	Os(3)	Os(1)	59.95(5)
Os(3)	Os(1)	Os(2)	56.215(7)	Os(3)	Os(1)	Os(2)	56.13(4)
Os(2)	Pt(1)	Os(1)	63.396(8)	Os(2)	Pt(1)	Os(1)	61.93(6)
Pt(1)	Os(2)	Os(3)	93.09(1)	Pt(1)	Os(2)	Os(3)	92.96(8)
Pt(1)	Os(1)	Os(3)	87.102(9)	Pt(1)	Os(1)	Os(3)	87.26(7)
Os(1)	Os(2)	Pt(1)	59.645(8)	Os(1)	Os(2)	Pt(1)	59.95(5)
Pt(1)	Os(1)	Os(2)	56.960(8)	Pt(1)	Os(1)	Os(2)	58.12(5)

[a] Estimated standard deviations in the least significant figure are given in parentheses.

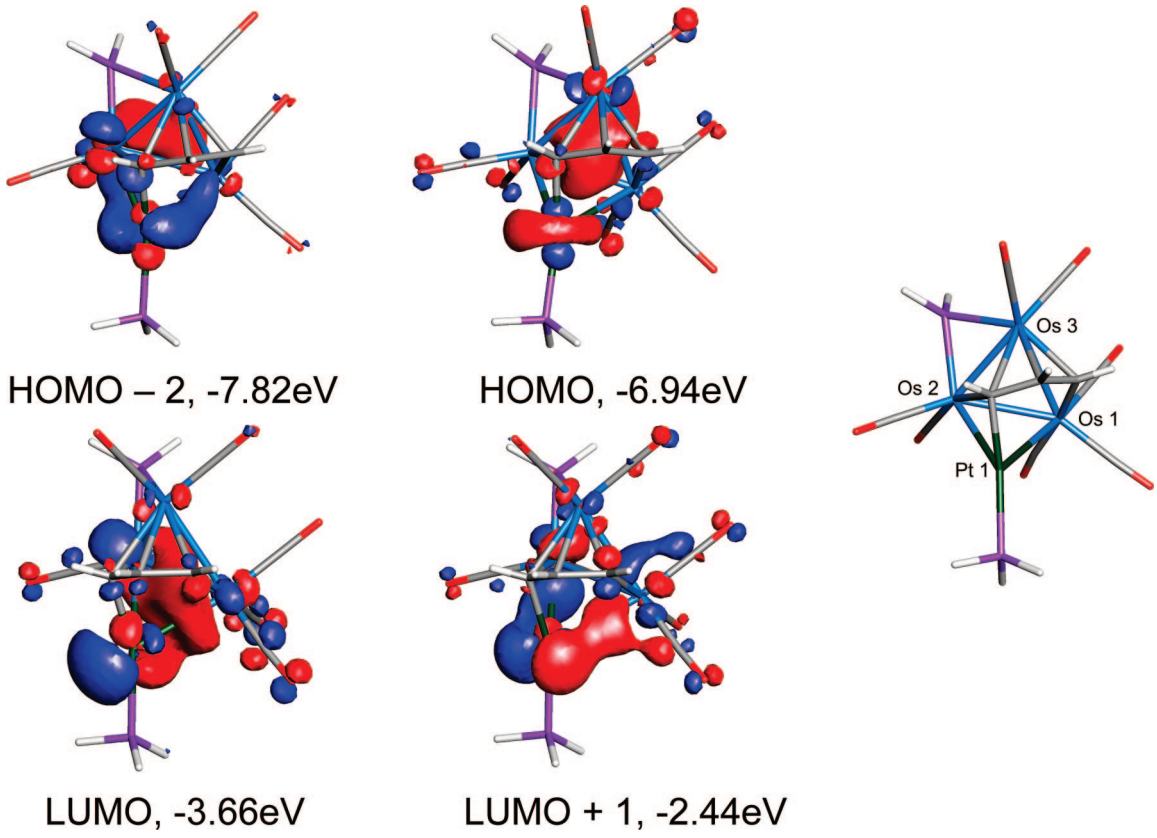

Figure 3. Contour diagrams of the Fenske–Hall frontier molecular orbitals of complex **3** with a stick diagram on the far right showing the approximate orientation of the molecule.

complex $Ru_5(CO)_{14}(\mu_4\text{-HCCPhCH})(\mu_3\text{-H})$.[20,21] In these two complexes both of the H-substituted carbon atoms are bonded to three metal atoms. The Pt−Os bond distances in **3** are slightly shorter than those in the planar Os_3Pt_n cluster complexes that we reported previously (eq 4):[5] Pt(1)−Os(1) = 2.7763(3) Å and Pt(1)−Os(2) = 2.6970(3) Å. The shortness of the Pt(1)−Os(2) bond can be attributed in part to the presence of the bridging carbon atom C(1).

As indicated by the ^{1}H NMR and mass spectra, there are no hydrido ligands present in **3**. The quadruply bridging CHC-MeCH ligand serves a 5-electron donor; thus, compound **3** contains a total of 58 cluster valence electrons and is thus electron-deficient by the amount of 4 electrons; an electronically saturated butterfly cluster of 4 metal atoms should have 62 valence electrons.[22] Accordingly, it was decided to investigate the electronic structure of **3** by computational methods.

To simplify the calculations, hydrogen atoms were substituted for the *tert*-butyl groups on the phosphorus atoms and for the methyl group on the dimetallallyl ligand. The Fenske–Hall frontier molecular orbitals for this model of **3** are shown in Figure 3. The highest occupied molecular orbital (HOMO) lies at –6.94 eV. This orbital is dominated by metal−metal bonding within the Os_3 triangle. The HOMO-2 at –7.82 eV consists of metal−metal bonding of the $PtOs_2$ group of metal atoms. The two lowest lying unoccupied molecular orbitals, the LUMO and LUMO+1, both lie at low energies: −3.66 and −2.44 eV, respectively. Thus, the molecule would benefit by having both of these orbitals filled with electrons, and if they were filled, the molecule would contain 62 cluster valence electrons. It should be noted that the LUMO and LUMO+1 both contain a significant component from the platinum atom, and this will

(20) Johnson, B. F. G.; Lewis, J.; McPartlin, M.; Nelson, W. J. H.; Raithby, P. R.; Sironi, A.; Vargas, M. D. *J. Chem. Soc., Chem. Commun.* **1983**, 1476–1477.

(21) Blake, A. J.; Dyson, P. J.; Gaede, P. E.; Johnson, B. F.G.; Parsons, S. *Organometallics* **1996**, *15*, 4100–4103.

(22) Mingos, D. M. P. *Acc. Chem. Res.* **1984**, *17*, 311–319.

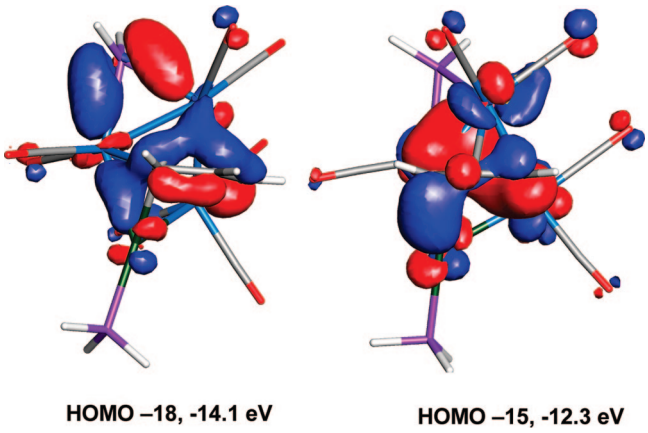

Figure 4. Contour diagrams of two of the Fenske–Hall molecular orbitals of **3** that show the bonding of the HCCMeCH ligand to the metal atoms.

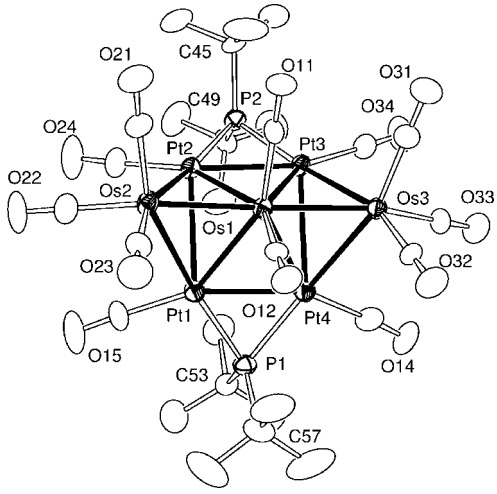

Figure 5. ORTEP diagram of **4** showing thermal ellipsoids at the 40% probability level. The hydrogen atoms on the methyl groups are omitted for clarity.

influence that reactivity of **3** that will be described below. To visualize the bonding of the bridging CHCMeCH ligand to the metal atoms, one must examine some of the molecular orbitals at significantly lower energies. Two of the key orbitals that exhibit this bonding are the HOMO-18 (–14.1 eV) and the HOMO-15 (–12.3 eV), which are shown in Figure 4. The delocalization of the bonding of the C_3 unit to metal atoms is readily apparent. The HOMO-18 shows the π-bonding of the entire C_3 unit to Os(3) and also the bonding of C(1) to the metal atoms Os(2) and Pt(1). The HOMO-15 shows what is effectively the σ-bonding of C(1) to Pt(1) and C(3) to Os(1).

An ORTEP diagram of the molecular structure of **4** is shown in Figure 5. Compound **4** contains seven metal atoms: four of platinum and three of osmium. The arrangement of the metal atoms could be described as a doubly capped square pyramid. Overall, it has approximate C_{2v} symmetry. The four platinum atoms define the square base, and one of the osmium atoms (Os(1)) occupies the apical position. The two capping groups are $Os(CO)_3$ groups: Os(2) and Os(3). Os(1) has two linear terminal carbonyl ligands. Each platinum atom has only one linear terminal carbonyl ligand. The molecule also contains two bridging di-*tert*-butylphosphido ligands. These were obviously formed by cleavage of a *tert*-butyl group from two PBu^t_3 ligands supplied by the $Pt(PBu^t_3)_2$. These ligands bridge the platinum atoms on opposite sides of the square base of the cluster. The PBu^t_2-bridged Pt−Pt bonds (Pt(1)−Pt(4) = 2.6567(7) Å and Pt(2)−Pt(3) = 2.6537(7) Å) are significantly shorter than the unbridged Pt−Pt bonds (Pt(1)−Pt(2) = 3.0390(8) Å and Pt(3)−Pt(4) = 3.1013(7) Å). The Os−Os bonds are unusually short (Os(1)−Os(2) = 2.6624(7) Å and Os(1)−Os(3) = 2.6613(7) Å) relative to the Os−Os distances found in $Os_3(CO)_{12}$.[16] This could be due to the lower number of carbonyl ligands on the osmium atoms in **4**, which would reduce the steric crowding around the metal atoms. Overall, compound **4** contains 94 cluster valence electrons. A doubly capped square pyramidal cluster of metal atoms should have 102 valence electrons.[22] The difference of 8 electrons could be rationalized by assuming that each of the four platinum atoms has only a 16-electron configuration.

In order to understand the electronic structure of **4**, its Fenske–Hall molecular orbitals were calculated. The frontiers orbitals for **4** are shown in Figure 6. The totally symmetrical A_1 HOMO lies at –5.2 eV. As can be seen by its contour diagram, this orbital involves an in-phase combination of contributions from all five metal atoms in the square-pyramidal cluster and also from the two capping osmium atoms. The A_2 LUMO lies at –4.1 eV, and nearly all metal−metal interactions are antisymmetric and antibonding. The bonding of the $Os(CO)_3$ capping groups to the cluster is shown nicely by the B_1 HOMO-1 (–6.5 eV) and the A_1 HOMO-4 (–8.8 eV) orbitals. This very effective metal−metal bonding may partially explain why the Os(1)−Os(2) and Os(1)−Os(3) bonds are so short.

At 150 °C, the yield of **3** (17%) increases at the expense of **2** (4%). The yield of **4** remains low (3%). In an independent experiment it was shown that compound **2** can be transformed into **3** and **4** in yields of 23% and 13%, respectively, when solutions of **2** were heated to reflux in decane solvent (174 °C) (eq 7). The transformation of the vinylidene ligand in **2** into the dimetallallyl ligand in **3** requires at least two CH activations on one of the methyl groups, and one of those hydrogen atoms must be shifted to the bridging carbon atom of the vinylidene ligand.

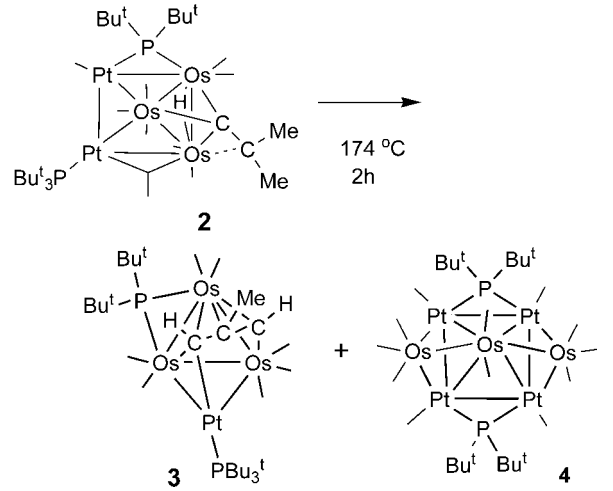

(7)

Because of its unusual electronic unsaturation, the reactivity of **3** toward CO was examined. Compound **3** was found to react with CO cleanly at room temperature to yield the complex $PtOs_3(CO)_8(PBu^t_3)(\mu\text{-}PBu^t_2)(\mu_4\text{-}CHCMeCH)$ (**5**) in 54% yield in 2 h. Compound **5** was characterized by a combination of IR and NMR spectroscopy, mass spectrometry, and single-crystal X-ray diffraction analysis. An ORTEP diagram of the molecular structure of **5** is shown in Figure 7. Selected intramolecular bond

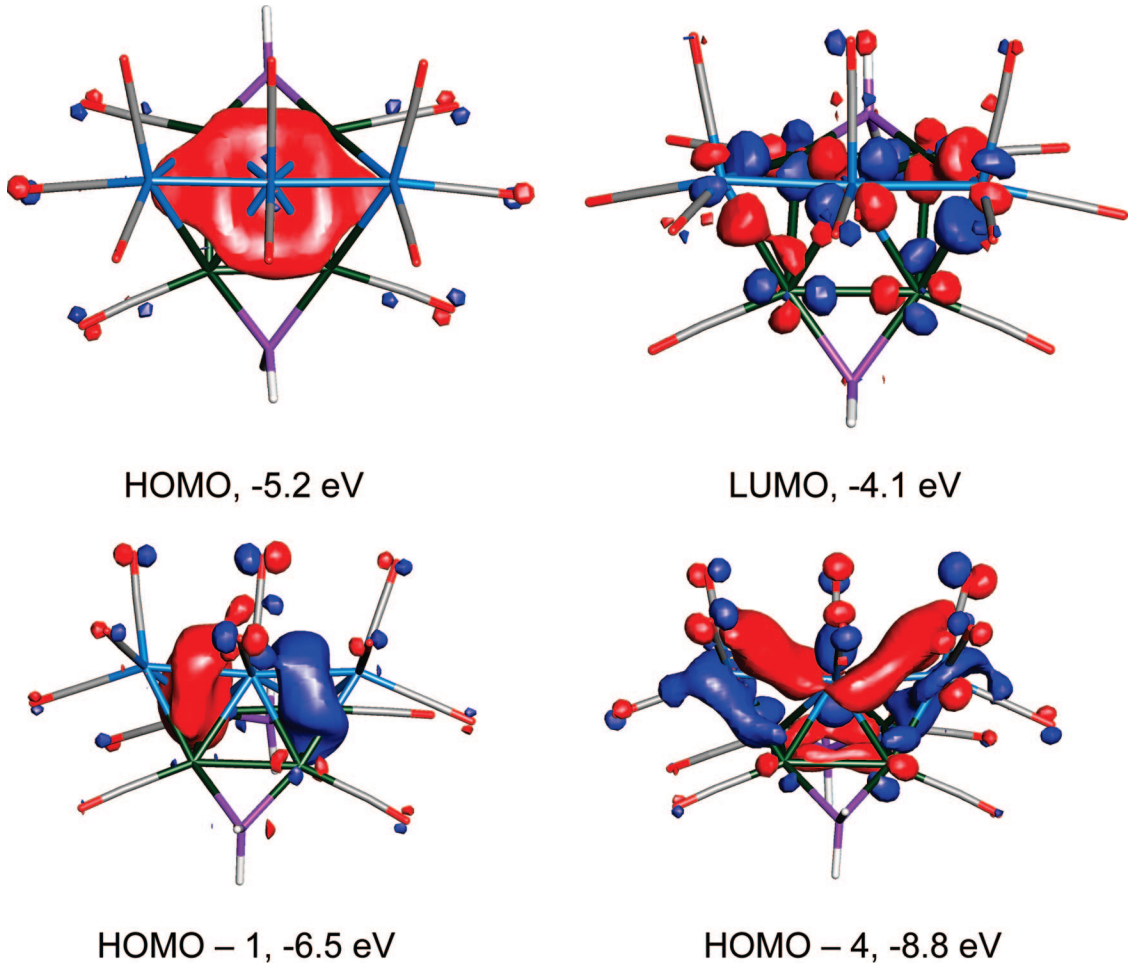

Figure 6. Contour diagrams of the Fenske–Hall molecular orbitals of **4** that show the nature of the metal−metal interactions in the metal cluster.

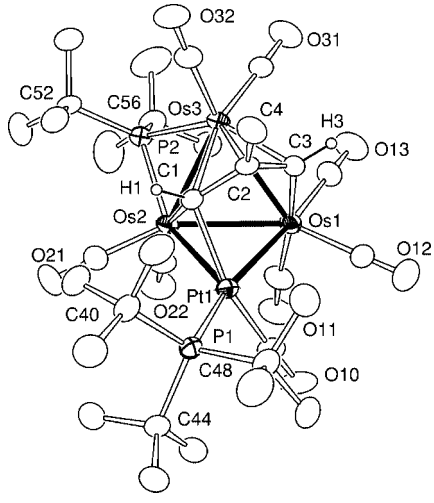

Figure 7. ORTEP diagram of **5** showing thermal ellipsoids at the 40% probability level. The hydrogen atoms on the methyl groups are omitted for clarity.

distances and angles for **3** and **5** are given in Tables 4 and 5, respectively. Compound **5** is structurally very similar to **3**, except that it contains one additional CO ligand. The added CO ligand (C(10)−O(10)) is coordinated to the platinum atom Pt(1) (Pt(1)−C(1) = 1.861(12) Å). The CO addition produced a slight increase in the lengths of the associated Pt−Os bonds relative to those in **3** (Pt(1)−Os(1) = 2.7915(6) Å and Pt(1)−Os(2) = 2.7384(6) Å). Interestingly, however, two of the Os−Os bonds in the Os_3 triangle (Os(1)−Os(2) = 2.8455(6) Å and Os(2)−Os(3) = 2.7279(5) Å) are slightly but significantly shorter than those in **3**. The long Os(1)−Os(3) bond in **3** is similarly long in **5** (2.9527(6) Å). In order to understand the effect of the CO addition, the Fenske–Hall molecular orbitals of **5** were calculated. The frontier MOs of **5** are shown in Figure 8. Compound **5** contains 60 cluster valence electrons, 2 electrons more than in **3**. Since the structures of **3** and **5** are very similar, it is easy to see that the filled HOMO in **5** (–6.75 eV) is very similar to the LUMO in **3** and the LUMO in **5** (–3.33 eV) is very similar to the LUMO+1 in **3**. Even though the LUMO+1 is still relatively energetically low, we found no evidence for the formation of a stable product formed by the addition of two CO ligands to **3**. The second CO addition to **3** might be inhibited by unfavorable steric crowding.

The addition of CO to **3** is partially reversible. When it was heated to 125 °C for 2 h in an octane solution, compound **5** released 1 equiv of CO and was converted back to **3** in 38% yield (eq 8).

Summary

Four new platinum−osmium compounds, **2**–**5**, have been obtained from reactions of $Os_3(CO)_{12}$ with $Pt(PBu^t_3)_2$ at elevated temperatures. All of the compounds contain bridging PBu^t_2 ligands formed by the cleavage of a *tert*-butyl group from a PBu^t_3 ligand. Aspects of the cleavage process were revealed in

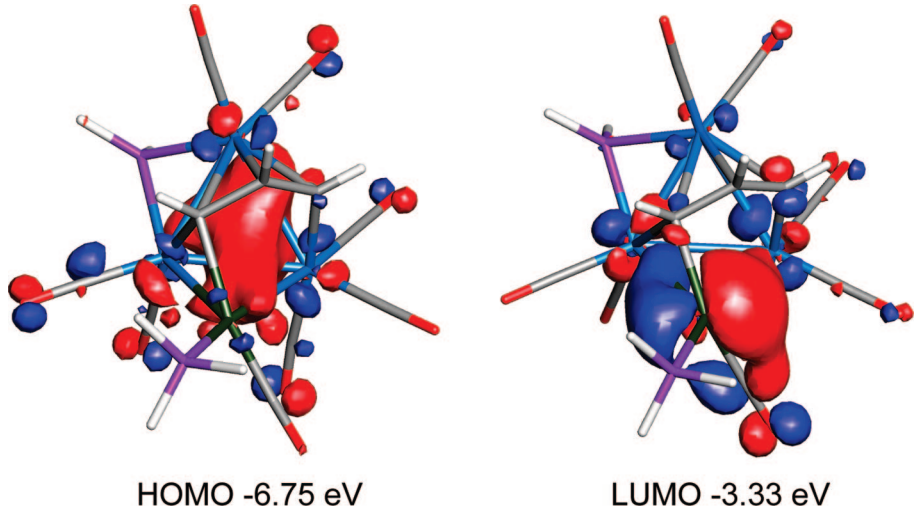

Figure 8. Contour diagrams of the Fenske–Hall HOMO and LUMO of **5**.

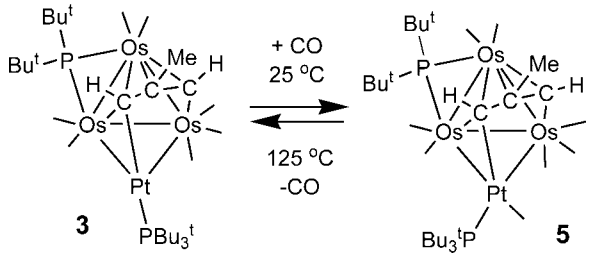

(8)

several of the compounds by the presence of a hydrocarbyl ligand fragment formed from a transformed *tert*-butyl group that remains coordinated to the cluster of metal atoms. The new products are electronically unsaturated, and one of them (**3**) was shown to add CO reversibly under mild conditions at its platinum atom.

Acknowledgment. This research was supported by the National Science Foundation under Grant No. CHE-0743190. We wish to thank Dr. Perry Pellechia for assistance with the NMR measurements and Dr. Mark Smith for assistance with the structural analyses.

Supporting Information Available: CIF files for each of the structural analyses. This material is available free of charge via the Internet at http://pubs.acs.org.

OM8000422